

Fuzzy Uncertainty Observer Based Filtered Sliding Mode Trajectory Tracking Control of the Quadrotor

Yong Wang¹, Ning Wang^{1(✉)}, Shuailin Lv¹, Jianchuan Yin²,
and Meng Joo Er^{1,3}

¹ Marine Engineering College, Dalian Maritime University, Dalian, China
15241192269@163.com, n.wang.dmu.cn@gmail.com, lvshuailin@gmail.com

² Navigation College, Dalian Maritime University, Dalian, China
yinjianchuan@gmail.com

³ School of EEE, Nanyang Technological University, Singapore, Singapore
emjer@ntu.edu.sg

Abstract. In this paper, a filtered sliding mode control (FSMC) scheme based on fuzzy uncertainty observer (FUO) for trajectory tracking control of a quadrotor unmanned aerial vehicle (QUAV) is proposed. To be specific, the dynamics model of QUAV is decomposed into three subsystems. By virtue of the cascaded structure, sliding-mode-based virtual control laws can be recursively designed. In order to remove the smoothness requirements on intermediate signals, a series of first-order filters are employed to reconstruct sliding mode control signals together with their first derivatives. Moreover, fuzzy uncertainty observers are employed to indirectly estimate lumped unknown nonlinearities including system uncertainties and external disturbances and make compensation for the QUAV system. Stability analysis and uniformly ultimately bounded tracking errors and states can be guaranteed by the Lyapunov approach. Simulation studies demonstrate the effectiveness and superiority of the proposed tracking control scheme.

Keywords: Quadrotor unmanned aerial vehicle · Trajectory tracking control · Sliding mode control · Fuzzy uncertainty observer

1 Introduction

Compared with traditional single rotor UAV, the most significant advantage of the quadrotor unmanned aerial vehicles (QUAV) is that the latter has better

N. Wang—This work is supported by the National Natural Science Foundation of P.R. China (under Grants 51009017 and 51379002), Applied Basic Research Funds from Ministry of Transport of P.R. China (under Grant 2012-329-225-060), China Postdoctoral Science Foundation (under Grant 2012M520629), the Fund for Dalian Distinguished Young Scholars (under Grant 2016RJ10), the Innovation Support Plan for Dalian High-level Talents (under Grant 2015R065), and the Fundamental Research Funds for the Central Universities (under Grant 3132016314).

stability, more compact structure and larger load, *etc.*. So the QUAV pertains to a wide area of possible applications including patrolling for forest fires, traffic monitoring, surveillance rescue, *etc.*, and as a remarkable platform for the UAV, the QUAV has been attracting numerous research [1–6].

The QUAV is a complex nonlinear strongly coupled system with more than one input and output, and thereby leading to great challenges in controller design and synthesis. In [7], PID control scheme is used to achieve the trajectory tracking control. However, this control method is classical linear control scheme, which only work better when the QUAV is near hovering state. Backstepping control scheme has an extensive application in controlling the QUAV in recent years. In [8], the QUAV dynamic system has been divided into two subsystems, i.e., translational subsystem and rotational subsystem and two subcontrollers have been designed. However, general backstepping control schemes need accurate model parameters and is not robust to model uncertainties and external disturbances, for this reason, adaptive integral backstepping control scheme [9] has been applied in the QUAV, which Only suitable for the model uncertainty and external disturbances are slow-varying or constant. Sliding mode control is a powerful control method with characteristics of simple and robust [10]. Combining with adaptive control strategy or observer [11], this kind control methods have widespread used various systems, however, chattering phenomenon is inevitable for the continuous switching logic. Adaptive fuzzy backstepping control has been used to the trajectory tracking control for the QUAV in [12], in which the fuzzy system is employed to approximate directly a model using backstepping techniques. For the reason of underactuation, the virtual controller is designed in most control schemes for the QUAV, while, the derivative of the virtual controller will be complex. In this context, we focus on a QUAV with the lumped unknown nonlinearity including system uncertainties and external disturbances, and a filtered sliding mode trajectory tracking control scheme based on fuzzy uncertainty observer (FUO) for the QUAV is proposed.

2 QUAV Dynamics and Problem Formulation

As shown in Fig. 1, defining the earth-fixed coordinate $OX_0Y_0Z_0$ and the body-fixed coordinate $O'XYZ$ which are respectively considered with the origin coinciding to the starting point and the gravity center of the QUAV. Vectors (x, y, z) and (ϕ, θ, ψ) are respectively denote the positions of the QUAV in earth-fixed coordinate $OX_0Y_0Z_0$ and the Euler angles in body-fixed coordinate $O'XYZ$, in which ϕ refers as to roll angle, θ refers as to pitch angle and ψ refers as to yaw angle.

The position dynamics can be described as follows:

$$\begin{cases} \dot{\boldsymbol{\eta}}_{11} = \boldsymbol{\eta}_{12} \\ \dot{\boldsymbol{\eta}}_{12} = \mathbf{f}_1(\boldsymbol{\eta}_{12}) + \mathbf{u}_1(\boldsymbol{\eta}_2, \tau) + \mathbf{d}_1(\boldsymbol{\eta}_{11}, \boldsymbol{\eta}_{12}, t) \end{cases} \quad (1)$$

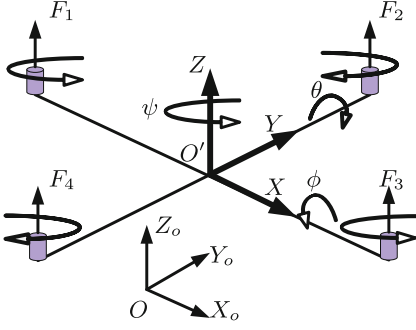


Fig. 1. The configuration of a QUAUV.

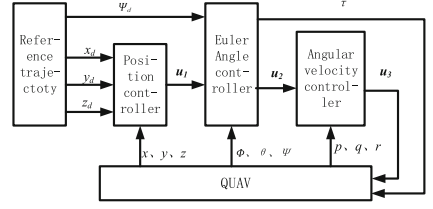


Fig. 2. The overall control diagram.

with the lumped model uncertainties and/or external disturbances $\mathbf{d}_1 = [d_{11}, d_{12}, d_{13}]^T$, $\mathbf{f}_1 = [D_x \dot{x}^2, D_y \dot{y}^2, D_z \dot{z}^2 - g]^T$ and

$$\mathbf{u}_1(\boldsymbol{\eta}_2, \tau) = \frac{\tau}{m} \begin{bmatrix} C_\phi S_\theta C_\psi + S_\phi S_\psi \\ C_\phi S_\theta S_\psi - S_\phi C_\psi \\ C_\phi C_\theta \end{bmatrix} \quad (2)$$

where $\boldsymbol{\eta}_{11} = [x, y, z]^T$ and $\boldsymbol{\eta}_{12} = [\dot{x}, \dot{y}, \dot{z}]^T$ are vectors of the positions and linear velocities in the earth-fixed frame, respectively, m is the mass of the QUAUV, g is the acceleration of the gravity, C_* and S_* are the functions $\cos(*)$ and $\sin(*)$, respectively, τ is the total thrust.

The vector of Euler angles $\boldsymbol{\eta}_2 = [\phi, \theta, \psi]^T$ is governed by

$$\dot{\boldsymbol{\eta}}_2 = \mathbf{g}_2(\boldsymbol{\eta}_2) \mathbf{u}_2(\boldsymbol{\eta}_3) + \mathbf{d}_2(\boldsymbol{\eta}_2, t) \quad (3)$$

with the lumped model uncertainties and/or external disturbances $\mathbf{d}_2 = [d_{21}, d_{22}, d_{23}]^T$, and

$$\mathbf{g}_2(\boldsymbol{\eta}_2) = \begin{bmatrix} 1 & S_\phi T_\theta & C_\phi T_\theta \\ 0 & C_\phi & -S_\phi \\ 0 & \frac{S_\phi}{C_\theta} & \frac{C_\phi}{C_\theta} \end{bmatrix} \quad (4)$$

$$\mathbf{u}_2(\boldsymbol{\eta}_3) = \boldsymbol{\eta}_3 \quad (5)$$

where T_* denotes the function $\tan(*)$, $\boldsymbol{\eta}_3 = [p, q, r]^T$ is the angular velocity vector in body-fixed coordinate given by the following dynamics:

$$\dot{\boldsymbol{\eta}}_3 = \mathbf{f}_3(\boldsymbol{\eta}_3) + \mathbf{g}_3 \mathbf{u}_3 + \mathbf{d}_3(\boldsymbol{\eta}_3, t) \quad (6)$$

with the diagonal matrix $\mathbf{g}_3 = \text{diag}(1/J_x, 1/J_y, 1/J_z)$ where J_i ($i = x, y, z$) is the moment of inertia with respect to each axis, $\mathbf{d}_3 = [d_{31}, d_{32}, d_{33}]^T$ include unmodeled dynamics and/or external disturbances, and $\mathbf{f}_3(\boldsymbol{\eta}_3) = [\frac{J_y - J_z}{J_x} qr, \frac{J_z - J_x}{J_y} pr, \frac{J_x - J_y}{J_z} pq]^T$, where $\mathbf{u}_3 = [u_{31}, u_{32}, u_{33}]^T$ is the control input and the final control input vector of the QUAUV system is $\mathbf{u} = [\tau, \mathbf{u}_3^T]^T$.

The control objective in this study is to design filtered sliding mode controller of the QUAV with FUO and achieve the trajectory tracking control ($x \rightarrow x_d, y \rightarrow y_d, z \rightarrow z_d, \psi \rightarrow \psi_d$) in presence of the external disturbances and system uncertainties. Before ending this section, the following assumption is introduced:

Assumption 1. *The desired trajectory and its time derivatives are bounded.*

3 Filtered Sliding Mode Controller Design

In this section, three subcontrollers will be designed. The overall control diagram is as shown in Fig. 2.

3.1 Position Controller

Given a reference trajectory $\boldsymbol{\eta}_{11d} := [x_d, y_d, z_d]^T$, combining with position dynamics (1), we design sliding surfaces as follows:

$$\mathbf{s}_{11}(t) = \mathbf{e}_{11}(t) + \mathbf{k}_{11} \int_0^t \mathbf{e}_{11}(\tau) d\tau \quad (7)$$

$$\mathbf{s}_{12}(t) = \mathbf{e}_{12}(t) + \mathbf{k}_{12} \int_0^t \mathbf{e}_{12}(\tau) d\tau \quad (8)$$

where $\mathbf{k}_{11} = \text{diag}(k_{111}, k_{112}, k_{113}) > 0$, $\mathbf{k}_{12} = \text{diag}(k_{121}, k_{122}, k_{123}) > 0$, $\mathbf{e}_{11} = \boldsymbol{\eta}_{11} - \boldsymbol{\eta}_{11d}$, $\mathbf{e}_{12} = \boldsymbol{\eta}_{12} - \bar{\boldsymbol{\eta}}_{12d}$, and $\bar{\boldsymbol{\eta}}_{12d}$ is the filtered output of the virtual control signal $\boldsymbol{\eta}_{12d}$ given by

$$\epsilon_1 \dot{\bar{\boldsymbol{\eta}}}_{12d} + \bar{\boldsymbol{\eta}}_{12d} = \boldsymbol{\eta}_{12d} \quad (9)$$

here, $\epsilon_1 > 0$ is an user-defined filtering time constant and let $\mathbf{y}_1 = \bar{\boldsymbol{\eta}}_{12d} - \boldsymbol{\eta}_{12d}$.

In this context, the virtual control signal $\boldsymbol{\eta}_{12d}$ can be selected as follows:

$$\boldsymbol{\eta}_{12d} = -\mathbf{p}_{11} \mathbf{s}_{11} + \dot{\boldsymbol{\eta}}_{11d} - \mathbf{k}_{11} \mathbf{e}_{11} - \mathbf{e}_{12} \quad (10)$$

where $\mathbf{p}_{11} = \text{diag}(p_{111}, p_{112}, p_{113}) > 0$ and a desired position control law for sub-system (1) can be designed as follows:

$$\mathbf{u}_1 = -\mathbf{p}_{12} \mathbf{s}_{12} - \mathbf{f}_1(\boldsymbol{\eta}_{12}) + \dot{\bar{\boldsymbol{\eta}}}_{12d} - \mathbf{k}_{12} \mathbf{e}_{12} - \hat{\mathbf{d}}_1 \quad (11)$$

with the FUO given by

$$\hat{\mathbf{d}}_1(\boldsymbol{\omega}_1 | \hat{\boldsymbol{\vartheta}}_1) = \hat{\boldsymbol{\vartheta}}_1^T \boldsymbol{\xi}_1(\boldsymbol{\omega}_1) \quad (12)$$

Choosing the parameter matrix update rule as

$$\dot{\hat{\boldsymbol{\vartheta}}}_1 = -r_{11} \hat{\boldsymbol{\vartheta}}_1 + r_{12} \boldsymbol{\xi}_1(\boldsymbol{\omega}_1) (\mathbf{s}_{12} + \boldsymbol{\varepsilon}_1)^T \quad (13)$$

where $r_{11} > 0$ and $r_{12} > 0$ are user-defined positive definite parameters, $\boldsymbol{\omega}_1 = [\boldsymbol{\eta}_{11}^T, \boldsymbol{\eta}_{12}^T]^T$ is the input vector of the fuzzy system, $\boldsymbol{\varepsilon}_1 = \boldsymbol{\eta}_{12} - \mathbf{v}_1$ is the observation error vector with

$$\dot{\mathbf{v}}_1 = -r_{13}\mathbf{v}_1 + \mathbf{f}_1(\boldsymbol{\eta}_{12}) + \mathbf{u}_1 + \hat{\mathbf{d}}_1(\boldsymbol{\omega}_1|\hat{\boldsymbol{\vartheta}}_1) + r_{13}\boldsymbol{\eta}_{12} \quad (14)$$

where $r_{13} > 0$ is user-defined positive definite parameter.

3.2 Euler Angle Controller

Substituting the control law (11) into the input nonlinearity (2), we can obtain

$$\begin{cases} \tau = m\|\mathbf{u}_1\| \\ \phi_d = \arcsin\left(\frac{m}{\tau}(S_{\psi_d}u_{11} - C_{\psi_d}u_{12})\right) \\ \theta_d = \arcsin\left(\frac{\frac{m}{\tau}u_{11} - S_{\psi_d}S_{\phi_d}}{C_{\psi_d}C_{\phi_d}}\right) \end{cases} \quad (15)$$

Let $\boldsymbol{\eta}_{2d} := [\phi_d, \theta_d, \psi_d]^T$ and $\bar{\boldsymbol{\eta}}_{2d} := [\bar{\phi}_d, \bar{\theta}_d, \bar{\psi}_d]^T$ where $\bar{\boldsymbol{\eta}}_{2d}$ is the filtered output of $\boldsymbol{\eta}_{2d}$ given by

$$\epsilon_2\dot{\bar{\boldsymbol{\eta}}}_{2d} + \bar{\boldsymbol{\eta}}_{2d} = \boldsymbol{\eta}_{2d} \quad (16)$$

here, $\epsilon_2 > 0$ is an user-defined filtering time constant and let $\mathbf{y}_2 = \bar{\boldsymbol{\eta}}_{2d} - \boldsymbol{\eta}_{2d}$.

Combining with Euler angles dynamics (3), we design a sliding surface as follows:

$$\mathbf{s}_2(t) = \mathbf{e}_2(t) + \mathbf{k}_2 \int_0^t \mathbf{e}_2(\tau) d\tau \quad (17)$$

where $\mathbf{e}_2 = \boldsymbol{\eta}_2 - \bar{\boldsymbol{\eta}}_{2d}$, $\mathbf{k}_2 = \text{diag}(k_{21}, k_{22}, k_{23}) > 0$.

In this context, a desired Euler angles control law for sub-system (3) can be designed as follows:

$$\mathbf{u}_2 = \mathbf{g}_2^{-1}(\boldsymbol{\eta}_2)[\dot{\bar{\boldsymbol{\eta}}}_{2d} - \mathbf{k}_2\mathbf{e}_2 - \mathbf{p}_2\mathbf{s}_2 + \mathbf{y}_2 - \hat{\mathbf{d}}_2] \quad (18)$$

with the FUO given by

$$\hat{\mathbf{d}}_2(\boldsymbol{\omega}_2 | \hat{\boldsymbol{\vartheta}}_2) = \hat{\boldsymbol{\vartheta}}_2^T \boldsymbol{\xi}_2(\boldsymbol{\omega}_2) \quad (19)$$

Choosing the parameter matrix update rule as

$$\dot{\hat{\boldsymbol{\vartheta}}}_2 = -r_{21}\hat{\boldsymbol{\vartheta}}_2 + r_{22}\boldsymbol{\xi}_2(\boldsymbol{\omega}_2)(\mathbf{s}_2 + \boldsymbol{\varepsilon}_2)^T \quad (20)$$

where $\mathbf{p}_2 = \text{diag}(p_{21}, p_{22}, p_{23}) > 0$, $r_{21} > 0$ and $r_{22} > 0$ are user-defined positive definite parameters, $\boldsymbol{\omega}_2 = [\boldsymbol{\eta}_2^T, \dot{\boldsymbol{\eta}}_2^T]^T$ is the input vector of the fuzzy system, $\boldsymbol{\varepsilon}_2 = \boldsymbol{\eta}_2 - \mathbf{v}_2$ is the observation error vector with

$$\dot{\mathbf{v}}_2 = -r_{23}\mathbf{v}_2 + \mathbf{g}_2(\boldsymbol{\eta}_2)\mathbf{u}_2 + \hat{\mathbf{d}}_2(\boldsymbol{\omega}_2|\hat{\boldsymbol{\vartheta}}_2) + r_{23}\boldsymbol{\eta}_2 \quad (21)$$

where $r_{23} > 0$ is user-defined positive definite parameter.

3.3 Angular Velocity Controller

Let $\boldsymbol{\eta}_{3d} := [p_d, q_d, r_d]^T = \mathbf{u}_2$, together with angular velocity dynamics (6), we design a sliding surface as follows:

$$\mathbf{s}_3(t) = \mathbf{e}_3(t) + \mathbf{k}_3 \int_0^t \mathbf{e}_3(\tau) d\tau \quad (22)$$

where $\mathbf{e}_3 = \boldsymbol{\eta}_3 - \bar{\boldsymbol{\eta}}_{3d}$, $\mathbf{k}_3 = \text{diag}(k_{31}, k_{32}, k_{33}) > 0$ and $\bar{\boldsymbol{\eta}}_{3d} := [\bar{p}_d, \bar{q}_d, \bar{r}_d]^T$ is the filtered output of $\boldsymbol{\eta}_{3d}$ given by

$$\epsilon_3 \dot{\bar{\boldsymbol{\eta}}}_{3d} + \bar{\boldsymbol{\eta}}_{3d} = \boldsymbol{\eta}_{3d} \quad (23)$$

here, $\epsilon_3 > 0$ is an user-defined filtering time constant and let $\mathbf{y}_3 = \bar{\boldsymbol{\eta}}_{3d} - \boldsymbol{\eta}_{3d}$.

Accordingly, an nominal angular velocity control law for sub-system (6) can be governed as follows:

$$\mathbf{u}_3 = \mathbf{g}_3^{-1} [\dot{\hat{\boldsymbol{\eta}}}_{3d} - \mathbf{f}_3(\boldsymbol{\eta}_3) - \mathbf{k}_3 \mathbf{e}_3 - \mathbf{p}_3 \mathbf{s}_3 + \mathbf{y}_3 - \hat{\mathbf{d}}_3] \quad (24)$$

with the FUO given by

$$\hat{\mathbf{d}}_3(\boldsymbol{\omega}_3 | \hat{\boldsymbol{\nu}}_3) = \hat{\boldsymbol{\nu}}_3^T \boldsymbol{\xi}_3(\boldsymbol{\omega}_3) \quad (25)$$

Choosing the parameter matrix update rule as

$$\dot{\hat{\boldsymbol{\nu}}}_3 = -r_{31} \hat{\boldsymbol{\nu}}_3 + r_{32} \boldsymbol{\xi}_3(\boldsymbol{\omega}_3) (\mathbf{s}_3 + \boldsymbol{\epsilon}_3)^T \quad (26)$$

where $\mathbf{p}_3 = \text{diag}(p_{31}, p_{32}, p_{33}) > 0$, $r_{31} > 0$ and $r_{32} > 0$ are user-defined positive definite parameters, $\boldsymbol{\omega}_3 = [\boldsymbol{\eta}_3^T, \dot{\boldsymbol{\eta}}_3^T]^T$ is the input vector of the fuzzy system, $\boldsymbol{\epsilon}_3 = \boldsymbol{\eta}_3 - \mathbf{v}_3$ is the observation error vector with

$$\dot{\mathbf{v}}_3 = -r_{33} \mathbf{v}_3 + \mathbf{f}_3(\boldsymbol{\eta}_3) + \mathbf{g}_3 \mathbf{u}_3 + \hat{\mathbf{d}}_3(\boldsymbol{\omega}_3 | \hat{\boldsymbol{\nu}}_3) + r_{33} \boldsymbol{\eta}_3 \quad (27)$$

where $r_{33} > 0$ is user-defined positive definite parameter.

Then, the final control law is

$$\mathbf{u} := \begin{bmatrix} \tau \\ \mathbf{u}_3 \end{bmatrix} = \begin{bmatrix} m \|\mathbf{u}_1\| \\ \mathbf{u}_3 \end{bmatrix} \quad (28)$$

4 Stability Analysis

Theorem 1. *Consider an uncertain QUAV system (1)–(3)–(6), together with control scheme (11), (18), (24) with FUO given by (12), (19), (25), all system states and signals and all tracking errors are globally uniformly ultimately bounded.*

Proof. Together with system (14), (21) and (27), we have

$$\dot{\boldsymbol{\varepsilon}}_i + r_{i3}\boldsymbol{\varepsilon}_i = \mathbf{d}_i - \hat{\mathbf{d}}_i(\boldsymbol{\omega}_i|\hat{\boldsymbol{\vartheta}}_i) \quad (29)$$

where $i = 1, 2, 3$.

Define the optimal parameter as

$$\boldsymbol{\vartheta}_i^* = \arg \min_{\hat{\boldsymbol{\vartheta}}_i \in M_{\boldsymbol{\vartheta}}_i} \left(\sup_{\boldsymbol{\omega}_i \in M_{\boldsymbol{\omega}}_i} \|\mathbf{d}_i - \hat{\mathbf{d}}_i\| \right) \quad (30)$$

where $M_{\boldsymbol{\vartheta}}_i$ and $M_{\boldsymbol{\omega}}_i$ are bounded sets.

Then we have

$$\mathbf{d}_i = \hat{\mathbf{d}}_i(\boldsymbol{\omega}_i|\boldsymbol{\vartheta}_i^*) + \boldsymbol{\zeta}_i(\boldsymbol{\omega}_i) \quad (31)$$

where $\boldsymbol{\zeta}_i(\boldsymbol{\omega}_i)$ is reconstruction error vector and $\|\boldsymbol{\zeta}_i(\boldsymbol{\omega}_i)\| < \bar{\zeta}_i$, $\bar{\zeta}_i > 0$. Let $\tilde{\boldsymbol{\vartheta}}_i = \boldsymbol{\vartheta}_i^* - \hat{\boldsymbol{\vartheta}}_i$, together with system (29), we can obtain

$$\dot{\boldsymbol{\varepsilon}}_i + r_{i3}\boldsymbol{\varepsilon}_i = \tilde{\boldsymbol{\vartheta}}_i^T \boldsymbol{\xi}_i(\boldsymbol{\omega}_i) + \boldsymbol{\zeta}_i(\boldsymbol{\omega}_i) \quad (32)$$

Combining with system (12), (19), (25), (31), the following equation holds

$$\mathbf{d}_i - \hat{\mathbf{d}}_i = \tilde{\boldsymbol{\vartheta}}_i^T \boldsymbol{\xi}_i(\boldsymbol{\omega}_i) + \boldsymbol{\zeta}_i(\boldsymbol{\omega}_i) \quad i = 1, \dots, 3 \quad (33)$$

then together with system (8), (17), (22) and (33), we can obtain

$$\begin{cases} \dot{\mathbf{s}}_{12} = -\mathbf{p}_{12}\mathbf{s}_{12} + \tilde{\boldsymbol{\vartheta}}_1^T \boldsymbol{\xi}_1(\boldsymbol{\omega}_1) + \boldsymbol{\zeta}_1(\boldsymbol{\omega}_1) \\ \dot{\mathbf{s}}_i = -\mathbf{p}_i\mathbf{s}_i + \mathbf{y}_i + \tilde{\boldsymbol{\vartheta}}_i^T \boldsymbol{\xi}_i(\boldsymbol{\omega}_i) + \boldsymbol{\zeta}_i(\boldsymbol{\omega}_i) \quad i = 2, 3 \end{cases} \quad (34)$$

Choosing the following Lyapunov function

$$V = \frac{1}{2} \left[\sum_{i=1}^3 \left(\mathbf{y}_i^T \mathbf{y}_i + \boldsymbol{\varepsilon}_i^T \boldsymbol{\varepsilon}_i + \frac{\text{tr}(\tilde{\boldsymbol{\vartheta}}_i^T \tilde{\boldsymbol{\vartheta}}_i)}{r_{i2}} \right) + \mathbf{s}_{11}^T \mathbf{s}_{11} + \mathbf{s}_{12}^T \mathbf{s}_{12} + \mathbf{s}_2^T \mathbf{s}_2 + \mathbf{s}_3^T \mathbf{s}_3 \right] \quad (35)$$

Together with system (32) and (34), the time derivative of (35) can be given as

$$\begin{aligned} \dot{V} = & \sum_{i=2}^3 \left(-\mathbf{s}_i^T \mathbf{p}_i \mathbf{s}_i + \mathbf{s}_i^T \mathbf{y}_i - r_{i3} \boldsymbol{\varepsilon}_i^T \boldsymbol{\varepsilon}_i + (\mathbf{s}_i^T + \boldsymbol{\varepsilon}_i^T) \boldsymbol{\zeta}_i(\boldsymbol{\omega}_i) + \mathbf{y}_i^T \dot{\mathbf{y}}_i \right) - \mathbf{s}_{11}^T \mathbf{p}_{11} \mathbf{s}_{11} \\ & + \mathbf{s}_{11}^T \mathbf{y}_1 - \mathbf{s}_{12}^T \mathbf{p}_{12} \mathbf{s}_{12} - r_{13} \boldsymbol{\varepsilon}_1^T \boldsymbol{\varepsilon}_1 + (\mathbf{s}_{12}^T + \boldsymbol{\varepsilon}_1^T) \boldsymbol{\zeta}_1(\boldsymbol{\omega}_1) + \mathbf{y}_1^T \dot{\mathbf{y}}_1 \\ & + \underbrace{\sum_{i=2}^3 \left((\mathbf{s}_i^T + \boldsymbol{\varepsilon}_i^T) \tilde{\boldsymbol{\vartheta}}_i^T \boldsymbol{\xi}_i(\boldsymbol{\omega}_i) - \frac{\text{tr}(\tilde{\boldsymbol{\vartheta}}_i^T \dot{\tilde{\boldsymbol{\vartheta}}}_i)}{r_{i2}} \right) + (\mathbf{s}_{12}^T + \boldsymbol{\varepsilon}_1^T) \tilde{\boldsymbol{\vartheta}}_1^T \boldsymbol{\xi}_1(\boldsymbol{\omega}_1) - \frac{\text{tr}(\tilde{\boldsymbol{\vartheta}}_1^T \dot{\tilde{\boldsymbol{\vartheta}}}_1)}{r_{12}}}_{M} \end{aligned} \quad (36)$$

together with systems (13), (20) and (26), we can obtain

$$\begin{aligned} M &= \sum_{i=2}^3 \left(\sum_{j=1}^3 (\tilde{\boldsymbol{\vartheta}}_{ij}^T ((s_{ij} + \varepsilon_{ij}) \boldsymbol{\xi}_i(\boldsymbol{\omega}_i) - \frac{\dot{\boldsymbol{\vartheta}}_{ij}}{r_{i2}})) \right) + \sum_{j=1}^3 (\tilde{\boldsymbol{\vartheta}}_{1j}^T ((s_{12j} + \varepsilon_{1j}) \boldsymbol{\xi}_1(\boldsymbol{\omega}_1) - \frac{\dot{\boldsymbol{\vartheta}}_{1j}}{r_{12}})) \\ &= \sum_{i=1}^3 \frac{r_{i1}}{r_{i2}} \text{tr}(\tilde{\boldsymbol{\vartheta}}_i^T \hat{\boldsymbol{\vartheta}}_i) \end{aligned} \quad (37)$$

where $\mathbf{s}_{12} = [s_{121}, s_{122}, s_{123}]^T$, $\mathbf{s}_i = [s_{i1}, s_{i2}, s_{i3}]^T$, $\boldsymbol{\varepsilon}_i = [\varepsilon_{i1}, \varepsilon_{i2}, \varepsilon_{i3}]^T$, $\tilde{\boldsymbol{\vartheta}}_i = [\tilde{\boldsymbol{\vartheta}}_{i1}, \tilde{\boldsymbol{\vartheta}}_{i2}, \tilde{\boldsymbol{\vartheta}}_{i3}]$ and $\dot{\boldsymbol{\vartheta}}_i = [\dot{\boldsymbol{\vartheta}}_{i1}, \dot{\boldsymbol{\vartheta}}_{i2}, \dot{\boldsymbol{\vartheta}}_{i3}]$ with $i = 1, 2, 3$.

Together with systems (9)–(10) and Assumption 1, we can obtain

$$\left\| \dot{\mathbf{y}}_1 + \frac{\mathbf{y}_1}{\varepsilon_1} \right\| \leq z_1(\dot{\mathbf{s}}_{11}, \ddot{\boldsymbol{\chi}}_{11d}, \dot{\mathbf{e}}_{11}, \dot{\mathbf{e}}_{12}) \quad (38)$$

where z_1 is continuous bounded function. Then, we have

$$\mathbf{y}_1^T \dot{\mathbf{y}}_1 \leq -\frac{\mathbf{y}_1^T \mathbf{y}_1}{\varepsilon_1} + \frac{1}{2} \mathbf{y}_1^T \mathbf{y}_1 + \frac{1}{2} z_1^2 \quad (39)$$

Similarly, there exists continuous bounded function $z_2(\cdot)$ and $z_3(\cdot)$, such that

$$\mathbf{y}_i^T \dot{\mathbf{y}}_i \leq -\frac{\mathbf{y}_i^T \mathbf{y}_i}{\varepsilon_i} + \frac{1}{2} \mathbf{y}_i^T \mathbf{y}_i + \frac{1}{2} z_i^2, \quad i = 2, 3 \quad (40)$$

In addition, using the Young's inequality, we have

$$\sum_{i=1}^3 \left(\frac{r_{i1}}{r_{i2}} \text{tr}(\tilde{\boldsymbol{\vartheta}}_i^T \hat{\boldsymbol{\vartheta}}_i) \right) \leq \sum_{i=1}^3 \left(\frac{r_{i1}}{2r_{i2}} \text{tr}(\boldsymbol{\vartheta}_i^{*T} \boldsymbol{\vartheta}_i^*) - \frac{r_{i1}}{2r_{i2}} \text{tr}(\tilde{\boldsymbol{\vartheta}}_i^T \tilde{\boldsymbol{\vartheta}}_i) \right) \quad (41)$$

Substituting system (37), (39), (40) and (41) into system (36), it is easy to obtain

$$\begin{aligned} \dot{V} &\leq \sum_{i=2}^3 \left(-\mathbf{s}_i^T (\mathbf{p}_i - \mathbf{I}) \mathbf{s}_i - \left(\frac{1}{\varepsilon_i} - 1 \right) \mathbf{y}_i^T \mathbf{y}_i - \left(r_{i3} - \frac{1}{2} \right) \boldsymbol{\varepsilon}_i^T \boldsymbol{\varepsilon}_i - \frac{r_{i1}}{2r_{i2}} \text{tr}(\tilde{\boldsymbol{\vartheta}}_i^T \tilde{\boldsymbol{\vartheta}}_i) \right) \\ &\quad - \mathbf{s}_{11}^T \left(\mathbf{p}_{11} - \frac{\mathbf{I}}{2} \right) \mathbf{s}_{11} - \mathbf{s}_{12}^T \left(\mathbf{p}_{12} - \frac{\mathbf{I}}{2} \right) \mathbf{s}_{12} - \left(r_{13} - \frac{1}{2} \right) \boldsymbol{\varepsilon}_1^T \boldsymbol{\varepsilon}_1 - \left(\frac{1}{\varepsilon_1} - 1 \right) \mathbf{y}_1^T \mathbf{y}_1 \\ &\quad - \frac{r_{11}}{2r_{12}} \text{tr}(\tilde{\boldsymbol{\vartheta}}_1^T \tilde{\boldsymbol{\vartheta}}_1) + \sum_{i=1}^3 \left(\bar{z}_i^2 + \frac{r_{i1}}{2r_{i2}} \text{tr}(\boldsymbol{\vartheta}_i^{*T} \boldsymbol{\vartheta}_i^*) + \frac{\bar{z}_i^2}{2} \right) \end{aligned} \quad (42)$$

where $\bar{z}_i(t)$ is the upper bound value of $z_i(t)$.

Selecting the following design parameters

$$\mathbf{p}_j \geq \frac{2 + \alpha}{2} \mathbf{I}, \frac{1}{\varepsilon_i} \geq 1 + \frac{\alpha}{2}, \mathbf{p}_{11} \geq \frac{1 + \alpha}{2} \mathbf{I}, \mathbf{p}_{12} \geq \frac{1 + \alpha}{2} \mathbf{I}, r_{i3} \geq \frac{1 + \alpha}{2}, \frac{r_{i1}}{r_{i2}} \geq \alpha$$

with $j = 2, 3$ and $i = 1, \dots, 3$, we have

$$\dot{V} \leq -\alpha V + C \quad (43)$$

with

$$C = \sum_{i=1}^3 \left(\bar{\zeta}_i^2 + \frac{r_{i1}}{2r_{i2}} \text{tr}(\boldsymbol{\theta}_i^* T \boldsymbol{\theta}_i^*) + \frac{\bar{z}_i^2}{2} \right) \quad (44)$$

Together with the system (35) and (42), the following inequality holds

$$0 \leq V(t) \leq V(0)e^{-\alpha t} + (1 - e^{-\alpha t}) \frac{C}{\alpha} < \infty \quad (45)$$

It is obvious that the function $V(t)$ is bounded and together with system (35), we can find that the trajectory error \mathbf{e}_{11} and the other error signals are uniformly ultimately bounded.

5 Simulation Studies

In this section, the effectiveness of the proposed control scheme for the QUAUV is evaluated. The lumped uncertainties and/or external disturbances are given by $\mathbf{d}_i(t) = 3[\sin t, \cos t, \sin t]^T + 0.1\boldsymbol{\eta}_i$, where $\boldsymbol{\eta}_1 = \boldsymbol{\eta}_{11} + \boldsymbol{\eta}_{12}$, $i = 1, 2, 3$.

The reference tracking trajectory is given as $[x_d, y_d, z_d, \psi_d] = [-2 \sin t/2, 2 \cos t/2, 2 \sin t + 3, \sin t]$ and the initial conditions of the QUAUV are set as follows: $x(0) = 2$, $y(0) = -0.5$, $z(0) = 2$, $\phi(0) = 1$.

Figure 3 shows the tracking of three positions and the yaw, where FSMC denotes the proposed filtered sliding mode control scheme and SMC denotes the traditional sliding mode control scheme. From Fig. 3 we can find that both the proposed control scheme and the SMC scheme are able to robustly stabilize the

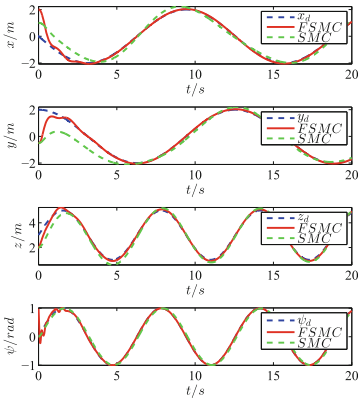


Fig. 3. States of x , y , z and ψ .

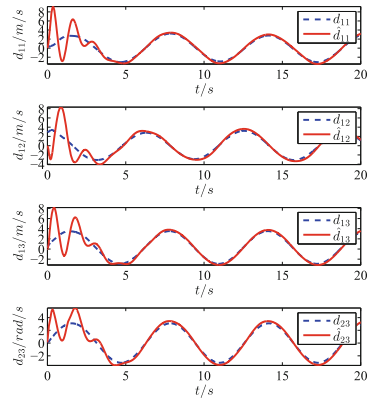


Fig. 4. Unknown nonlinearities.

QUAV and make it track the desired trajectory, while it is obvious that the proposed control scheme has faster response and higher accuracy. Figure 4 shows the estimate state of the FOU for the lumped unknown nonlinearities including system uncertainties and external disturbances on the trajectory, i.e., x , y , z and the yaw ψ , from which we can see, although the unknown lumped nonlinearities continuous change along with the time, FOU can estimate the unknown nonlinearities well. In summary, we can conclude that the proposed tracking control approach can achieve remarkable performance in terms of tracking accuracy and disturbance rejection.

6 Conclusion

In this paper, a filtered sliding mode control scheme based on FOU for trajectory tracking of a QUAV has been proposed. To be specific, three cascaded sub-controllers are designed by incorporating underactuation constraints. First-order filters are employed to reconstruct sliding mode control signals together with their first derivatives, and thereby decoupling the iterative design within the QUAV tracking control scheme. Furthermore, FOUs have been designed to estimate the lumped unknown nonlinearities. By the Lyapunov approach, we have proven that all system states and signals and tracking errors are globally uniformly ultimately bounded. Simulation studies have demonstrated the effectiveness and superiority of the proposed tracking control scheme.

References

1. Cabecinhas, D., Naldi, R., Silvestre, C., Cunha, R., Marconi, L.: Robust landing and sliding maneuver hybrid controller for a quadrotor vehicle. *IEEE Trans. Control Syst. Technol.* **24**(2), 400–412 (2016)
2. Driessens, S., Pounds, P.: The triangular quadrotor: a more efficient quadrotor configuration. *IEEE Trans. Robot. Autom.* **31**(6), 1517–1526 (2015)
3. Elfeky, M., Elshafei, M.: Quadrotor with tiltable rotors for manned applications. In: *Proceedings of the 11th International Systems, Signals and Devices Multi-Conference*, pp. 1–5 (2004)
4. Mohd, B., Mohd, A., Husain, A.R., Danapalasingam, K.A.: Nonlinear control of an autonomous quadrotor unmanned aerial vehicle using backstepping controller optimized by particle swarm optimization. *J. Eng. Sci. Technol. Rev.* **8**(3), 39–45 (2015)
5. Jiang, J., Qi, J.T., Song, D.L., Han, J.D.: Control platform design and experiment of a quadrotor. In: *Proceedings of the Chinese Control Conference*, pp. 2974–2979 (2013)
6. Sadeghzadeh, I., Mehta, A., Chamseddine, A., Zhang, Y.M.: Active fault tolerant control of a quadrotor UAV based on gainscheduled PID control. In: *Proceedings of the IEEE Canadian Conference on Electrical and Computer Engineering*, pp. 1–4 (2012)
7. Ortiz, J.P., Minchala, L.I., Reinoso, M.J.: Nonlinear robust H-Infinity PID controller for the multivariable system quadrotor. *IEEE Lat. Am. Trans.* **14**(3), 1176–1183 (2016)

8. Rashad, R., AbouDonia, A., Ayman, E.B.: Backstepping trajectory tracking control of a quadrotor with disturbance rejection. In: Proceedings of the XXV International Information, Communication and Automation Technologies (ICAT) Conference, pp. 1–7 (2015)
9. Zheng, F., Gao, W.N.: Adaptive integral backstepping control of a Micro-Quadrotor. In: Proceedings of the International Intelligent Control and Information Conference, pp. 910–915 (2011)
10. Runcharoon, K., Srichatrapimuk, V.: Sliding Mode Control of quadrotor. In: Proceedings of the International Conference on Technological Advances in Electrical, Electronics and Computer Engineering (TAECE), pp. 552–557 (2013)
11. Besnard, L., Shtesscl, Y.B., Landrum, B.: Quadrotor vehicle control via sliding mode control driven by sliding mode disturbance observer. *J. Franklin Inst.* **349**(2), 658–684 (2012)
12. Yacef, F., Bouhali, O., Hamerlain, M.: Adaptive fuzzy backstepping control for trajectory tracking of unmanned aerial quadrotor. In: Proceedings of the International Conference on Unmanned Aircraft Systems (ICUAS), pp. 920–927 (2014)